EARTHQUAKE ENGINEERING AND STRUCTURAL DYNAMICS
Earthquake Engng Struct. Dyn. 2011; **40**:887–902
Published online 17 November 2010 in Wiley Online Library (wileyonlinelibrary.com). DOI: 10.1002/eqe.1065

Performance-based earthquake engineering assessment of a self-centering, post-tensioned concrete bridge system

Won K. Lee[1,*,†,‡] and Sarah L. Billington[2,§]

[1]*Forell/Elsesser Engineers, San Francisco, CA 94111, U.S.A.*
[2]*Department of Civil and Environmental Engineering, Stanford University, Stanford, CA 94305, U.S.A.*

SUMMARY

Highway bridges in highly seismic regions can sustain considerable residual displacements in their columns following large earthquakes. These residual displacements are an important measure of post-earthquake functionality, and often determine whether or not a bridge remains usable following an earthquake. In this study, a self-centering system is considered that makes use of unbonded, post-tensioned steel tendons to provide a restoring force to bridge columns to mitigate the problem of residual displacements. To evaluate the proposed system, a code-conforming, case-study bridge structure is analyzed both with conventional reinforced concrete columns and with self-centering, post-tensioned columns using a formalized performance-based earthquake engineering (PBEE) framework. The PBEE analysis allows for a quantitative comparison of the relative performance of the two systems in terms of engineering parameters such as peak drift ratio as well as more readily understood metrics such as expected repair costs and downtime. The self-centering column system is found to undergo similar peak displacements to the conventional system, but sustains lower residual displacements under large earthquakes, resulting in similar expected repair costs but significantly lower expected downtimes. Copyright © 2010 John Wiley & Sons, Ltd.

Received 27 June 2009; Revised 10 August 2010; Accepted 12 August 2010

KEY WORDS: residual displacements; performance-based earthquake engineering; post-tensioned concrete; self-centering; highway structures

INTRODUCTION

In recent years, the earthquake engineering community has been focusing attention on performance-based design in order to predict and manage better the post-earthquake functionality and condition of structures. Excessive direct and indirect monetary losses due to non-structural damage and downtime that were sustained in recent earthquakes (e.g. Kobe 1995, Northridge 1995, Loma Prieta 1989) revealed that the philosophy of designing only for life safety (i.e. collapse prevention) under very large earthquakes was not sufficient in meeting the diverse needs of structure owners and of society as a whole. Performance-based design is an alternative approach wherein the goal is to incorporate a pre-defined level of post-earthquake performance into the design of a structure such that the damage is kept to 'acceptable' levels, with the definition of acceptable varying on the type and use of a structure.

The use of performance-based design to achieve post-earthquake functionality of critical structures is most commonly thought of as applied to building structures (e.g. hospitals, fire stations).

*Correspondence to: Won K. Lee, Forell/Elsesser Engineers, San Francisco, CA 94111, U.S.A.
†E-mail: wonlee21@gmail.com
‡Structural Engineer.
§Associate Professor.

However, managing the post-earthquake functionality of bridge structures can be equally important. Many highway bridges are critical links in the transportation network, and they must remain unbroken so that emergency services can be provided immediately following an earthquake. In addition, the uninterrupted function of the transportation network is crucial to maintaining normal societal function. Standard highway bridges in highly seismic regions such as California are typically designed such that plastic behavior will concentrate in the columns during earthquakes. The columns are expected to undergo large inelastic deformations under severe earthquakes, which can result in permanent, or residual, displacements. These residual displacements are an important measure of post-earthquake functionality in bridges, and can determine whether or not a bridge remains usable following an earthquake. For example, following the Kobe earthquake, over 100 reinforced concrete (RC) columns with a residual drift ratio (displacement normalized by column height) of over 1.5% were demolished even though they did not collapse [1]. Research has also shown residual displacements to be a key indicator of the ability of structures damaged in an earthquake to resist aftershocks [2–4].

In this study, a self-centering system is considered for bridge columns to mitigate the problem of residual displacements. The system makes use of unbonded, post-tensioned steel tendons to provide a restoring force to the columns, thereby reducing residual displacements and allowing for immediate operability of bridge structures following a large earthquake. To assess possible benefits of reduced residual displacements on bridge structures, the self-centering system is compared with a conventional RC system using a formalized, performance-based earthquake engineering (PBEE) framework. With the use of the PBEE framework, the performance of the two systems is compared and the applicability of the system is evaluated.

SUMMARY OF PEER PBEE ASSESSMENT METHODOLOGY

The methodology for PBEE used in this study was developed by the Pacific Earthquake Engineering Research Center (PEER) and encompasses four main steps: hazard analysis, structural analysis, damage analysis, and loss analysis. Each step is handled on an individual basis and in a probabilistic fashion. All of the steps are then combined to provide an assessment of overall system performance in terms of metrics such as monetary losses, downtime, and casualties. A complete description of this approach can be found in, for example, Moehle and Deierlein [5]. The four steps are briefly summarized here and are shown graphically in Figure 1:

1. *Hazard Analysis*: Given a site location and structural design, perform a Probabilistic Seismic Hazard Analysis to calculate the annual frequency with which a given seismic Intensity Measure (IM), e.g. spectral acceleration, will exceed certain levels (expressed with a hazard curve).

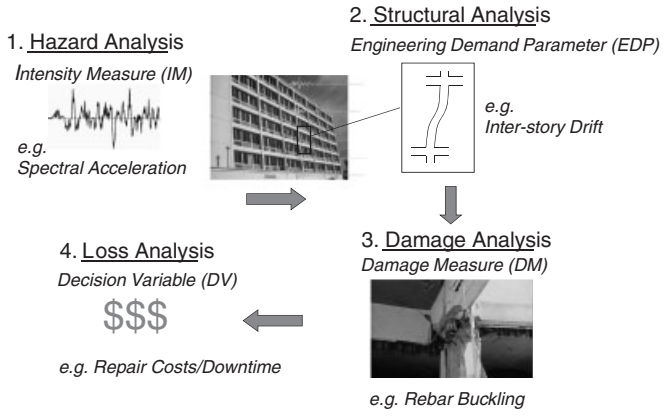

Figure 1. Performance-based earthquake engineering framework.

DOI: 10.1002/eqe

2. *Structural Analysis*: Given the IM and the structural design, perform simulations on models of the structure to determine resulting Engineering Demand Parameters (EDPs), which are measures of the structural response to the given IM. EDPs include such values as drift ratios, floor accelerations, and plastic hinge rotations.
3. *Damage Analysis*: Given the EDP, determine the probability that a structural component or system will experience a certain level of damage. The levels of damage are defined by damage states or damage measures (DMs) particular to the system under consideration. Examples of DMs include concrete cover spalling and reinforcing bar buckling.
4. *Loss Analysis*: Given the levels of damage sustained, calculate measures of performance termed Decision Variables (DVs), which can be used by owners of a structure for decision making. DVs are typically given in terms of monetary losses, structure or facility downtime, or casualties.

The previously described steps can be represented in the form of an equation based on the total probability theorem as follows:

$$v(DV) = \iiint G\langle DV|DM\rangle \cdot |\mathrm{d}G\langle DM|EDP\rangle| \cdot |\mathrm{d}G\langle EDP|IM\rangle| \cdot |\mathrm{d}\lambda(IM)| \tag{1}$$

where $v(DV)$ is the mean annual frequency of exceeding a certain DV, and for example $G\langle DV|DM\rangle$ is the complementary cumulative distribution function (CDF) of DV conditioned on DM.

BENCHMARK BRIDGE

The design of the bridge used in this study was performed by engineers at the California Department of Transportation (Caltrans) according to the Caltrans Bridge Design Specifications and Seismic Design Criteria (SDC) [6]. The bridge was one of a set of bridges designed to represent the majority of RC highway overpass bridges in California, and full details of the design and assumptions are given in Ketchum *et al.* [7]. The geometry and configuration of the bridge are shown in Figure 2. Factors such as skew, variable columns heights, and varying soil/foundation conditions were not considered in these analyses. While a specific site was not considered during the actual design of the bridge by Ketchum *et al.* [7], the bridge was assumed to be located within 10 km (6.2 miles) of the Hayward Fault, and was designed assuming a stiff soil site (Caltrans SDC Soil Class D). The superstructure has five spans and was designed as a cast-in-place, post-tensioned concrete box girder with a width of 11.9 m (39 ft) to carry two lanes of traffic. The inner three spans are 45.7 m (150 ft) and the outer two spans are 36.6 m (120 ft). The superstructure concrete was assumed to have an unconfined compressive strength of 34.5 MPa (5 ksi).

The bridge has four single-column bents, where each column is 15.2 m (50 ft) tall and has a diameter of 1.8 m (72 in). The column concrete was assumed for the design to have an unconfined compressive strength of 27.6 MPa (4 ksi). The longitudinal reinforcement is 52 #36 (#11 U.S.) bars in bundles of two bars, which corresponds to a reinforcing ratio of 1.9%. The transverse reinforcement is #22 (#7 U.S.) spirals with a center-to-center spacing of 8.26 cm (3.25 in), corresponding to a volumetric reinforcing ratio of 1.1%.

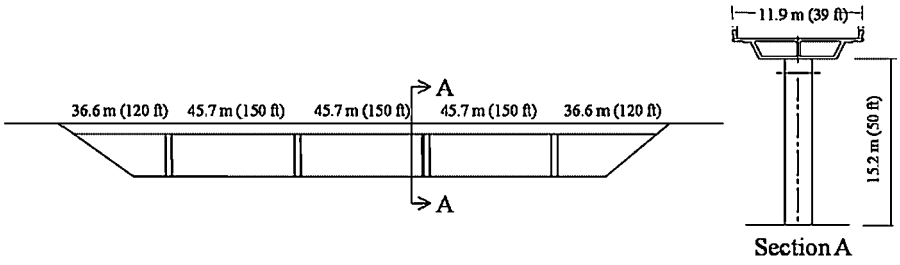

Figure 2. Bridge configuration and geometry.

DOI: 10.1002/eqe

BENCHMARK BRIDGE WITH SELF-CENTERING COLUMNS

To compare the self-centering system with the conventional RC system, the same bridge was used, except that the RC columns were replaced with self-centering columns that use unbonded post-tensioning (UBPT). A goal of the UBPT design is that the column size, stiffness, and strength remain similar to the conventional RC column, such that the reductions in residual displacements and subsequent improvement to post-earthquake functionality could be directly compared between the two systems. Sakai and Mahin [8–10] demonstrated through numerical and experimental investigations that by adding a concentric, post-tensioned tendon to a circular concrete column while also reducing the bonded longitudinal reinforcing, a column with similar yield strength and initial stiffness as the original column could be obtained that displayed self-centering behavior. Sakai and Mahin [8, 9] found that if roughly half of the area of bonded, mild steel longitudinal reinforcing was removed and an equivalent area of post-tensioned reinforcement was added, the self-centering behavior could be achieved while maintaining a stiffness and strength similar to that of the original column.

Using Sakai and Mahin's recommendation as a starting point, a series of cyclic analyses (described in a following section) were performed by varying the amounts of bonded mild steel and unbonded post-tensioned steel to determine the values that would allow for self-centering while maintaining a strength and stiffness similar to that of the original column. The resulting design used a post-tensioned tendon with an area of 200 cm^2 (31 in^2) and a prestress of 689 MPa (100 ksi).

In addition to reducing bonded reinforcement when adding the post-tensioned reinforcement, Sakai and Mahin [8, 9] also recommended increasing the spiral reinforcement to increase the compressive strength and ductility of the concrete to account for the increased axial load from the post-tensioned steel. The unconfined compressive strength of the concrete was increased from 27.6 MPa (4 ksi) to 56.2 MPa (8 ksi) for the UBPT column design, and the amount of confinement was increased to provide additional ductility. In the final design, the longitudinal reinforcing ratio was 0.9% (24 equally spaced #36 [#11 U.S.] bars) and the transverse volumetric reinforcing ratio was 1.4% (#25 [#8 U.S.] spirals at a spacing of 8.26 cm).

HAZARD ANALYSIS

To perform the hazard analysis, a site was selected that was within 10 km of the Hayward Fault and on stiff soil, as per the original RC bridge design. The site chosen for the bridge was in Oakland, California, with a latitude and longitude of 37.80 N × 122.30 W. The IM considered in this study was the spectral acceleration at the first mode period, $S_a(T_1)$, or simply S_a. In this research, a commercially available software package was used to perform the Probabilistic Seismic Hazard Analysis, using the Abrahamson and Silva [11] attenuation model to obtain the S_a hazard curve for the site. Based on an eigenvalue analysis of a numerical model of the structure (further discussed in following sections), a fundamental period of 1 second was assumed for both bridge structures. The S_a hazard curve for the site is shown in Figure 3.

STRUCTURAL ANALYSIS

The bridge was modeled using the open-source structural analysis software OpenSees (opensees.berkeley.edu). A schematic representation of the bridge model is shown in Figure 4. The model was three-dimensional, allowing two horizontal components of the ground motion to be used in the analysis. The vertical component of motion was not used in the analysis. The bridge was modeled using fiber elements. The skeleton of the bridge model (superstructure elements and abutments) was created for related studies on performance-based assessment of various bridge systems [12].

DOI: 10.1002/eqe

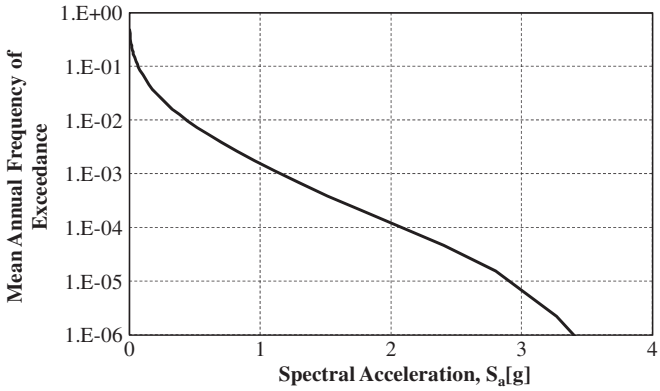

Figure 3. Spectral acceleration hazard curve for Oakland site.

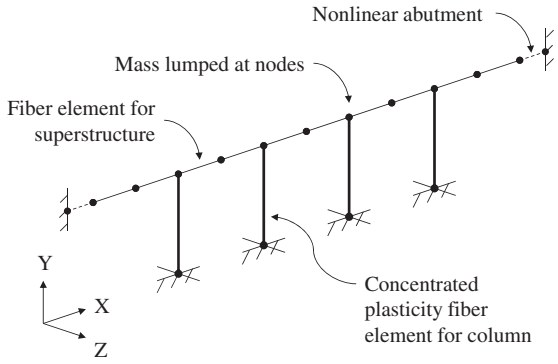

Figure 4. Schematic representation of bridge model.

The superstructure was modeled with flexibility-based, fiber beam–column elements. Each span was modeled with two elements. No significant nonlinear behavior was expected to occur in the superstructure. Mass due to the weight of the superstructure and the columns was lumped at the element end nodes. The abutments were modeled using spring elements that incorporated the behavior of the bearing pads, backfill, and backwall. The overall range of movement in the longitudinal direction was restricted by the backwall, and because of the stiffness provided by the abutments, the motion in the longitudinal direction was not expected to be as significant as the motion in the transverse direction.

Each column was modeled with a single, concentrated plasticity fiber beam–column element, as shown in Figure 5. The element is not a concentrated plasticity element in the conventional sense, wherein the nonlinear behavior is concentrated into moment-rotation springs at the ends of an element. Rather, the element is a fiber-based element with nonlinear constitutive behavior limited to specified plastic hinge regions at the ends of the element. The remainder of the element behaves linear elastically. Full details of the element formulation are given in Scott and Fenves [13]. The cracked stiffness values for the elastic region of the beam and the plastic hinge length were computed using Caltrans SDC [6] recommendations. For the analyses herein, soil–structure–foundation interaction is not considered and the columns are assumed fixed at the base.

As stated earlier, the column concrete was assumed to have an unconfined compressive strength of 27.6 MPa (4 ksi). For the core concrete, the peak compressive stress and strain were increased due to the confinement effect based on Mander *et al.* [14]. The fiber section was discretized into core and cover fibers, where the unconfined concrete values were used for the cover fibers and the confined concrete values were used for the core fibers. The Kent–Scott–Park model [15] was used to model concrete cover fiber behavior. Previous studies using fiber element models [9, 16, 17] to

DOI: 10.1002/eqe

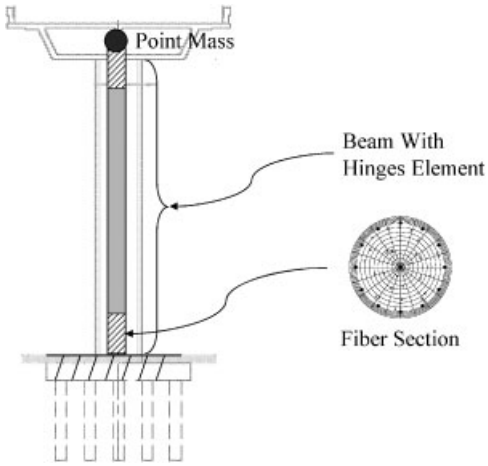

Figure 5. Schematic representation of column model.

simulate dynamically loaded RC columns have shown that the fiber element models have difficulty capturing residual displacements. For improved residual displacement prediction based on a study by Lee and Billington [18], a modified Kent–Scott–Park model developed for improved residual displacement prediction in RC columns was used to model the confined concrete fibers. The modified model allows the stress-strain path of the concrete to reload at a different point then the point of initial unloading when it moves into regions of high tensile strains. The model was based on calibration to shake-table testing of RC columns [10, 17].

The bonded mild steel reinforcing was assumed to have a yield strength of 469 MPa (68 ksi), given in the Caltrans SDC [6] as the *Expected Yield Strength* of Grade 60 reinforcing steel. The stress–strain relationship for the bonded mild steel reinforcement was assumed to follow the Giuffre-Menegotto-Pinto model [19], which incorporates the Bauschinger effect for cyclic loading. Strain hardening at 2% of the initial elastic modulus was assumed. An eigenvalue analysis of the bridge model yielded a first mode period of approximately 1.1 seconds, and the mode shape of this period corresponded to motion in the transverse direction of the bridge.

The UBPT column was modeled similarly to the RC column, with the addition of a truss element to model the post-tensioned tendon. The method of modeling the UBPT columns was validated against shake-table testing of UBPT columns by Sakai *et al.* [10], and is presented in Lee and Billington [20]. The truss element was modeled as elastic with a prescribed initial strain to apply the prestress. The low initial prestress of 690 MPa (100 ksi) was intentionally selected to prevent yielding of the PT tendon under seismic loading. The results from a cyclic analysis for each column design (RC and UBPT) are shown in Figure 6.

The ground motion record set used for the dynamic analysis is shown in Table I. The set consisted of 17 records assembled from record sets prepared by Somerville and Collins [21] and Tothong (P. Tothong, personal communication, 2006). A deagreggation of the PSHA results for $S_a(T_1)$ at the site in this study revealed that the majority of the contribution to the seismic hazard at the site results from events with short source-to-site distances (on the order of 10 km), as expected for a site that lies so close to a major fault. Thus a ground motion set consisting of near-fault motions was selected for this study, and such a set would be expected to be applicable to many of the bridges in California in general, which are located close to major faults.

The dynamic analyses were performed using the fault normal and fault parallel components of motion for each record. In the analyses, the fault normal component (generally the more severe of the two components) was applied in the transverse direction of the bridge, as motion in the longitudinal direction was expected to be limited by the presence of the abutments. Geometric nonlinearity was included in all analyses. Rayleigh damping was applied with a damping ratio of 2% specified at the first two structure modes. An additional 10 s of free vibration (analysis with

DOI: 10.1002/eqe

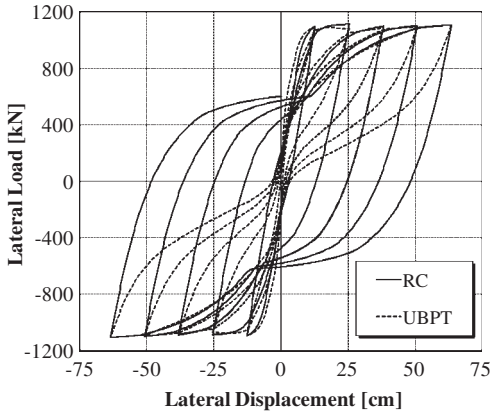

Figure 6. Cyclic analysis of RC and UBPT columns for baseline bridge.

Table I. Ground motion set for PBEE analysis.

No.	Earthquake	Magnitude	Station	Distance (km)
1	Erzincan, Turkey	6.7	Erzincan	1.8
2	Kobe, Japan	6.9	Kobe JMA	0.5
3	Loma Prieta	7.0	Corralitos	3.4
4	Loma Prieta	7.0	Gavilan	9.5
5	Loma Prieta	7.0	Gilroy Historic	12.7
6	Loma Prieta	7.0	Lexington Dam	6.3
7	Loma Prieta	7.0	Los Gatos Pres. Center	3.5
8	Loma Prieta	7.0	Saratoga Aloha Ave.	8.3
9	Tottori, Japan	6.6	Kofu	10.0
10	Tottori, Japan	6.6	Hino	1.0
11	Superstition Hills	6.5	El Centro Imp. Co. Cent.	18.2
12	Superstition Hills	6.5	Parachute Test Site	0.9
13	Loma Prieta	7.0	Gilroy Array #2	11.0
14	Loma Prieta	7.0	Gilroy Array #4	14.3
15	Northridge	6.7	Canoga Pk-Topanga Can	14.7
16	Northridge	6.7	Newhall-W.Pico Can. Rd.	8.0
17	Northridge	6.7	Sylmar-Olive View Med.	8.0

input acceleration of zero) was performed following the end of each ground motion to allow the bridge to come to rest such that residual displacements could be recorded.

The Incremental Dynamic Analysis (IDA) procedure [22] was performed by scaling the ground motions to increasing levels of S_a. In this study, the records were scaled based on the fault normal component of motion, and the same scale factor was applied to the fault parallel component as recommended by Somerville and Collins [21]. The IDA was performed at seven different intensity levels, which are shown in Table II.

The two EDPs considered to be of interest in the structural analysis were the peak drift ratio and the residual drift ratio at the top of the columns. The drift values were computed as the square root of the sum of the squares of the two orthogonal, horizontal directions of motion. Although the peak values were taken as the maximum of all four columns, the displacement responses of the four columns were similar due to the stiffness of the superstructure and the fact that the same acceleration history was applied uniformly to the bases of all of the columns.

The results from the IDA are shown in Figures 7 and 8. The resulting EDP values for each ground motion are shown at each intensity level (S_a). The computed median values (assuming that the EDP values are log-normally distributed) are shown with a solid line and the plus and minus one standard deviation values are shown with dashed lines. In Figure 7, a comparison is made between the peak drift ratios of the RC and the UBPT bridges. In general, the peak drifts for the

DOI: 10.1002/eqe

Table II. Intensity levels chosen for scaling of ground motions in IDA.

Level	Mean annual frequency of exceedance	$S_a(T_1)$ (g)
1	0.0139 (50% in 50 yrs)	0.36
2	0.0038	0.70
3	0.0021 (10% in 50 yrs)	0.91
4	0.0012	1.10
5	0.0007	1.30
6	0.0003 (2% in 50 yrs)	1.52
7	0.00025	1.70

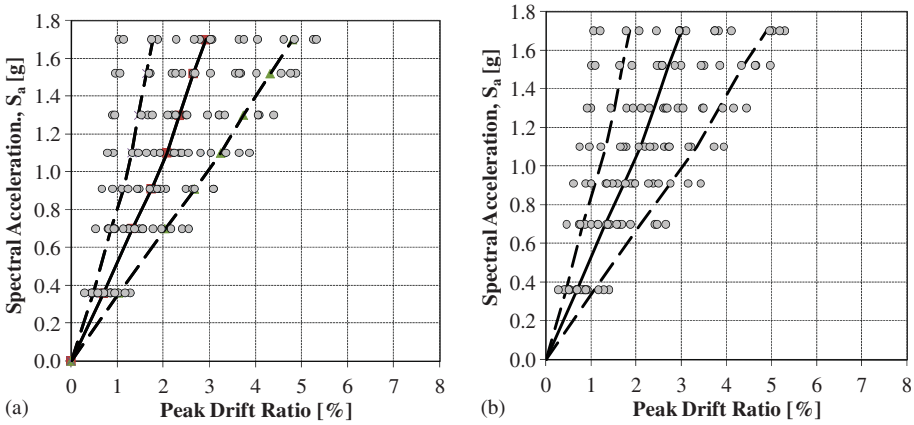

Figure 7. Comparison of peak drifts for bridge with (a) RC columns and (b) UBPT columns.

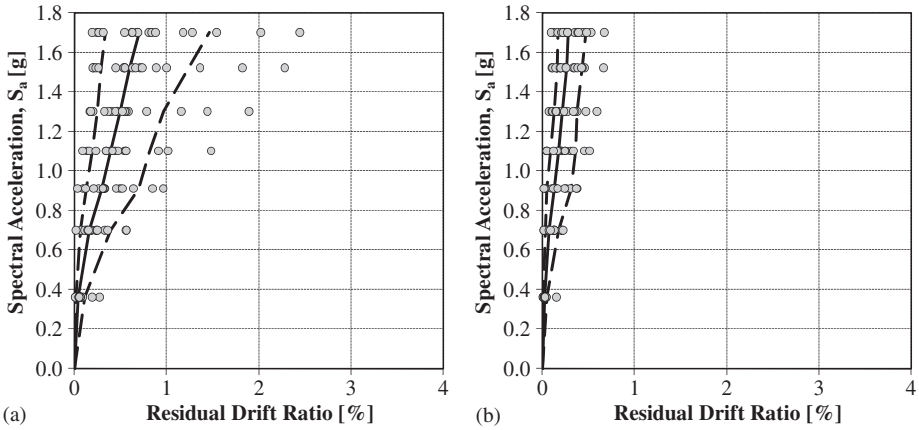

Figure 8. Comparison of residual drifts for bridge with (a) RC columns and (b) UBPT columns.

two systems are close for a given intensity level. The results contradict the notion that systems with lower hysteretic energy dissipation will have greater displacement demands than systems with a similar backbone curve but with more hysteretic energy dissipation. Although the IDA appears to be almost linear, the bridge itself does not remain in the elastic range.

The performance of the UBPT columns with respect to peak drift response was as desired, i.e. in the design of the UBPT columns, the goal was to proportion the columns such that the peak drift response would be similar to that of the RC columns. In this way, any expected damage in bridge components related to peak drifts would be comparable in the two systems and the UBPT

DOI: 10.1002/eqe

bridge would not produce additional damage that would make it disadvantageous compared with the RC system.

The magnitudes of the peak drifts of the bridges reflect a conservative design. At the 50% in 50 years IM level (S_a of $0.36g$), the median peak drift ratio of the two bridges was approximately 0.7%, which corresponds to a drift ratio that is within the elastic range. At the 2% in 50 years IM level (S_a of $1.52g$), the median peak drift ratio of the two bridges was roughly 2.6%, which corresponds to a ductility demand of less than 3. At this level of drift, yielding occurs in the columns, but the ductility demand is low enough that the safety of the structure would not be comprised. In the context of design based on current codes, the bridge meets expectations, as expected damage would be minimal under more frequent and less intense earthquakes, while collapse prevention would be successfully met under larger and less frequent earthquakes.

A comparison between the residual drift ratios of the RC and the UBPT bridges is shown in Figure 8. Unlike the peak drift response, there is a clear difference in the residual drift response of the two bridge systems. With increasing intensity, the bridge with RC columns begins to sustain significant residual displacements, with a large dispersion in the magnitudes of the residual displacements for the different ground motions. On the other hand, the bridge with UBPT columns retains substantially lower residual displacements with increasing intensity, with much less dispersion in the results.

At the 50% in 50 years IM level (S_a of $0.36g$), the median residual drift ratio of the RC columns is approximately 0.1%, while the median residual drift ratio of the UBPT columns is approximately 0.04%. This magnitude of residual displacements for both column systems is low enough that both bridges would likely be considered usable following an earthquake. At the 2% in 50 years IM level, a weakness in the RC column system is exposed. For the RC column system, four of the records led to residual displacements in the columns greater than 1%, and the median residual drift was 0.6% with plus/minus one standard deviation values of 0.29 and 1.24%, respectively. In the cases where the residual drift ratio exceeds 1%, the functionality of the bridge in this state would be questionable. For the UBPT column system, the median residual drift ratio at the 2% in 50 years hazard level was 0.25% with plus/minus one standard deviation values of 0.15 and 0.42%, respectively. In no case did any of the records lead to a residual drift ratio of greater than 1%, and the maximum value was 0.67%. These lower residual drift ratios sustained by the UBPT column would likely leave the bridge in an operational state following an earthquake.

From the hazard and structural analyses, the performance of the two bridge systems has been evaluated in terms of response parameters of interest to structural engineers (e.g. drift). To translate this response for non-engineers (e.g. in terms of metrics such as expected repair costs or downtime), the remaining two steps of the PBEE analysis are conducted as follows.

DAMAGE ANALYSIS

The results from the structural analyses are next used to predict the levels of expected damage in the structure using fragility functions as will be explained here. The damage states considered for the bridge were assumed to be related to the column EDPs only, as the columns are the elements in which most of the damage is expected to occur. Damage in the columns was assumed to be manifested in three forms, which were: (1) spalling of the cover concrete, (2) presence of residual displacements, and (3) buckling of longitudinal reinforcing bars. These three forms of damage were expected to represent the dominant forms of damage in tall, flexure-dominated columns such as the ones in this study. Spalling of cover concrete corresponds to a minor damage state, where the column is in usable condition but requires relatively minor repair. Residual displacements represent a state in which the column has undergone significant nonlinear behavior (e.g. yielding of mild steel) and may still be operational depending on the level of residual displacement. Buckling of longitudinal reinforcement corresponds to a severe level of damage, where major repair or even total replacement would be required. The same three forms of damage were assumed

DOI: 10.1002/eqe

to be appropriate for both the conventional RC columns as well as the self-centering, UBPT columns.

Typically, damage states selected in the PEER framework are discrete, meaning that they are assumed either to happen or not to happen. An example of such a discrete damage state is punching shear in an RC slab-column connection. In the case of the spalling of cover concrete and buckling of longitudinal reinforcing, the amount of spalled concrete area and the number of bars that buckle can vary. However, for this study, these two states are assumed to be discrete (e.g. either spalling occurs, or it does not).

Residual displacements, on the other hand, could be considered a continuous value rather than a discrete state, as any value is possible. However, a low residual displacement may not significantly affect the functionality of a bridge. Therefore, to maintain consistency in the sense of using discrete damage states, the damage state associated with residual displacements is defined here as having two states. Below a threshold value the bridge is assumed to be functional and above it the bridge would be considered unusable. If the bridge had a residual displacement that exceeded the threshold value, it would have to be demolished and replaced; thus the damage state will be henceforth referred to as *replacement level residual displacement*. Again, this damage state is not easily broken down into a simple 'yes' or 'no' state, and the decision to deem a bridge unusable due to residual displacements would have to be made by an engineer at the site.

To relate structural response to damage, fragility functions are used. The fragility functions give the probability of a structure or component being in a discrete damage state given the structural response (EDP). Fragility functions are typically based on experimental data, and in the case of RC columns, a large amount of data exists for use in this type of damage analysis. Berry and Eberhard [23] developed empirical fragility curves for RC columns. In their study, a large database of cyclic tests on RC columns was compiled, and statistical analyses were performed on the data to develop predictive equations for two damage modes in RC columns, which were cover concrete spalling and longitudinal bar buckling. Equations for estimating the mean drift at which spalling or bar buckling would occur, along with values of the variance of the predictions, were developed as a function of axial load ratio, length, diameter, and longitudinal reinforcing ratio. These equations are used to predict the likelihood of spalling and bar buckling in the columns in this study.

Using the mean and standard deviation values from the Berry and Eberhard equations and assuming a log-normal distribution, fragility curves were created using the CDF of the distribution. In the case of these two damage states of spalling and bar buckling, the EDP in the fragility curve is the peak drift ratio. The fragility curves for these two damages states for both columns are shown in Figure 9. From basic mechanics of prestressed concrete, the effect of a concentric UBPT tendon on a column is an increase in the axial load in the column. Thus the fragility equations were assumed to be applicable to both the RC and the UBPT columns, as the increase in axial load

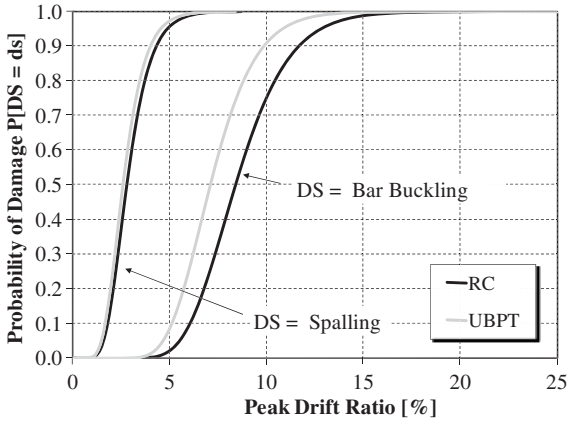

Figure 9. Fragility curves for spalling and bar buckling damage states.

DOI: 10.1002/eqe

due to the prestress in the UBPT columns is accounted for explicitly in the predictive equations. The mean drift ratio values for spalling and bar buckling for the RC column were computed to be 2.8 and 8.4%, respectively. Similarly, the mean drift ratio values for spalling and bar buckling for the UBPT column were computed as 2.6 and 7.1%, respectively.

For the damage state of replacement level residual displacements, the fragility curve cannot be created in the same way as for the spalling and bar buckling damage states for two reasons. First, the decision that a bridge is no longer usable due to excessive residual displacements is subjective. Two different engineers may give opposing recommendations for the same damaged column. In addition, although the residual displacement will be a primary factor, the decision will likely be based on additional observable damage, such as spalling and cracking in the column and damage to other components. The second reason is that much less data exist for this type of damage state. The type of data that could be used is the actual decisions made on replacing columns following past earthquakes.

A fragility curve for the damage state of excessive residual displacements is developed here based on engineering judgment and recently adopted Japanese bridge design guidelines. To create the fragility curve, an EDP that is closely related to the damage is first identified, and then a relationship between the magnitude of the EDP and the presence of the damage state is assumed. The EDP was chosen to be the residual displacement itself. This is an EDP that is obtained directly from the analysis, and is a direct measure of whether a bridge could be deemed unusable.

The fragility curve was then assumed to be a linear function. A limit of residual displacement was assumed after which a bridge would be deemed unusable no matter the conditions of the other components of the bridge. This limiting value was assumed based on the newly adopted Japanese code for highway bridge design [24]. In this code, a limit of 1.5% residual drift following an earthquake is placed on the design of new highway bridges. For residual drifts below this limiting value, the bridge may still be considered unusable due to the combination of some residual displacement and other observed damage in the bridge. For this study, it is assumed that residual drifts greater than 1% may be considered large enough to warrant replacement depending on other damage in the bridge. Therefore, a linear function, ranging from 1 to 1.5% drift, was adopted for the fragility curve, as shown in Figure 10. The residual displacement fragility curve is assumed to be applicable to both the RC and UBPT columns. While the fragility curve in Figure 10 is based on many assumptions that deserve attention for future validation, it serves the purpose of providing a method of comparing two different systems. The sensitivity of the final results to the choice of assumed fragility curve can be assessed with a sensitivity analysis as was performed and is reported in Lee and Billington [20].

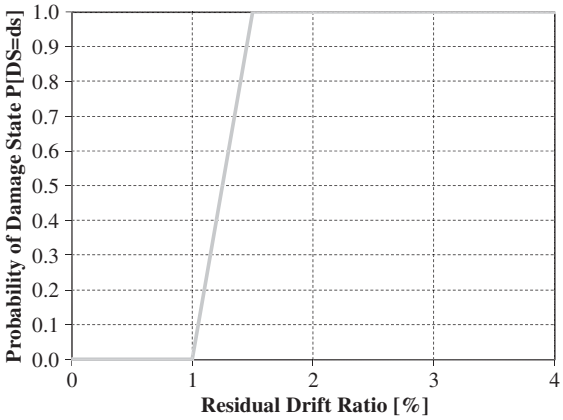

Figure 10. Fragility curve for excessive residual displacement damage state.

DOI: 10.1002/eqe

LOSS ANALYSIS

The fourth and final portion of PEER's PBEE assessment is to compute DVs for the structure given the expected levels of damage obtained from the previous steps. These DVs allow engineers, owners, and in general any decision makers to easily compare and assess structures in terms that are comprehensible to all parties. Examples of DVs are 'dollars, downtime, and deaths' (e.g. Porter [25]). The DVs considered to be most applicable to highway bridges are dollars, i.e. repair or replacement costs for damaged components, and downtime, i.e. the time that is required to bring the structure back to an operational state either through repair or replacement of the entire structure. Expected repair and replacement costs are a clear choice for comparison of alternative structures in the case of any type of structure. In the case of highway bridges in particular, downtime is a good choice because the loss of functionality of important links in the transportation network could be devastating following an earthquake.

Damage in typical highway bridges during an earthquake can occur in numerous components. Mackie *et al.* [26] compiled and processed damage and cost data from Caltrans statistics and post-earthquake case histories [27, 28] to estimate the expected costs for damage of various bridge components. They found that damage for the bridge type in this study primarily consists of damage to the columns, expansion joints, bearings, back walls, shear keys, approach slabs, and deck. The damage in all of these components except the columns will be similar for the two bridges as they are primarily based on peak displacements, which were found to be similar for the two bridge systems. Therefore, in this study, where the goal is to compare two systems rather than assess individual systems, only costs due to columns are considered.

The repair cost and downtime mean and standard deviation values for the damages states are given in Table III. For the damage state of spalling, Mackie *et al.* [26] reported the cost of repair to be a function of the square footage of spalled concrete. Specifically, a cost of \$100 per square foot is given. The damage models do not give expected areas of spalled concrete, but rather give whether a column has experienced spalling or not. An estimation must be made of the area of spalling that occurs in the columns if spalling occurs. For the sake of comparison, an approximation is made and used consistently between the two systems. The assumption is that if spalling occurs, it will occur along the entire plastic hinge length and around the entire circumference of the column. For the plastic hinge length value of 152 cm (60 in), this corresponds to an area of 8.76 m^2 (94.25 ft^2). For four columns, the total cost of repairing spalling if it occurs would therefore be \$37 700. A standard deviation of \$10 per square foot is assumed for the repair cost, giving a standard deviation in total repair cost for spalling of \$3,770. The mean and standard deviation values are assumed to be applicable to both the RC and UBPT bridge columns.

For the damage state of buckling of longitudinal reinforcement, the repair actions required are assumed to be replacement of longitudinal and spiral reinforcing, and addition of steel column casing based on Mackie *et al.* [26]. The cost of steel reinforcing and steel column casing is assumed to be \$2 per kilogram and \$2000 per linear foot, respectively, with standard deviations of \$0.20 and \$200, respectively. The amount of steel reinforcing to be replaced and the amount of steel casing required per column of this baseline bridge are assumed to be 1562 kg and 50 linear feet, respectively [26]. For four columns, the total cost of repairing the columns in the buckling damage state is therefore \$412 500, with a standard deviation of \$40 020.

Table III. Damage states and assumed repair costs and downtime.

Damage state	Mean repair cost	Std. Dev. repair cost	Mean downtime	Std. dev. downtime
Spalling	\$37,780	\$3,770	0	0
Bar Buckling	\$412,500	\$40,020	0	0
Residual Drift				
• RC Columns	0	0	75	42
• PT Columns	0	0	90	42

DOI: 10.1002/eqe

The damage state of spalling is assumed to be repairable without loss of functionality of the bridge, i.e. the bridge can remain operational while repairs are made. While some loss of functionality may be expected while repairing bar buckling damage depending on the severity downtime due to the possibility of excessive bar buckling is not considered here. Therefore, the two damage states of spalling and bar buckling correspond only to repair costs and do not have any associated downtimes.

For the damage state of excessive residual displacements, repair is unlikely (due to the difficulty of 'straightening' deformed bridges), leaving demolition and replacement of the entire bridge as the primary option. In the case where the bridge is no longer usable and must be demolished, there is an associated cost for replacement, but this cost is considered of secondary importance as compared with the actual downtime of a bridge. For this reason, as well as to simplify the analysis by decoupling this damage state from the previous two damage states, only downtime losses are considered when considering the excessive residual drift damage state. Although costs related to repairing damage from residual displacements that do not lead to bridge replacement could be considered in addition to downtime, they are not considered here as they are not critical to an evaluation of post-earthquake functionality.

The HAZUS99 SR2 Technical Manual [29] is used to obtain rough estimates of downtime for the damage state of excessive residual displacements. The HAZUS Manual presents mean values for restoration times for highway bridges. The damage state of replacement-level residual displacement is assumed to correspond to the extensive damage state in HAZUS99. The state of extensive damage for bridges in HAZUS is 'defined by any column degrading without collapse—shear failure—(column structurally unsafe), significant residual movement at connections, or major settlement approach, vertical offset at abutment, differential settlement at connections, shear key failure at abutments' [29]. The mean restoration time, or downtime, for a highway bridge in the extensive damage state is reported as 75 days with a standard deviation of 42 days. This value is for a standard bridge and likely would not apply to the UBPT bridge. To be conservative, a 20% longer mean restoration time, i.e. 90 days, with the same standard deviation of 42 days is assumed to represent the possibility of additional construction time needed for the cast-in-place, post-tensioned columns.

INTEGRATION OF ANALYSIS RESULTS: PBEE ASSESSMENT

The results from the four steps of the PEER PBEE analysis were combined using the framing integral of Equation (1) to generate repair cost and downtime hazard curves, shown in Figures 11 and 12, respectively. For a given mean annual frequency of exceedance, the repair cost for the UBPT system is slightly higher than that of the RC system. The slightly higher repair cost for the UBPT system was expected, as the repair costs are based on peak drift values, which in the

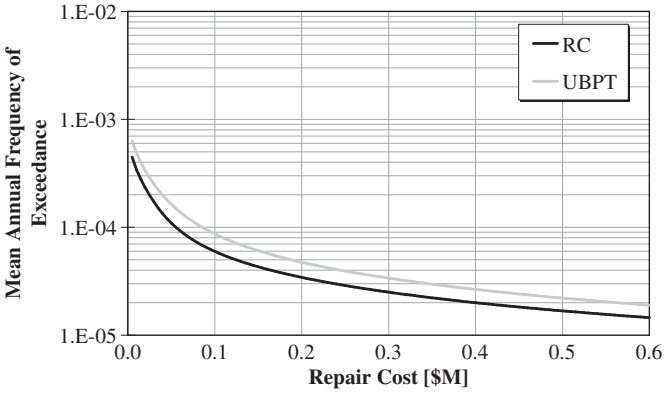

Figure 11. Hazard curves for peak-drift-related repair costs.

DOI: 10.1002/eqe

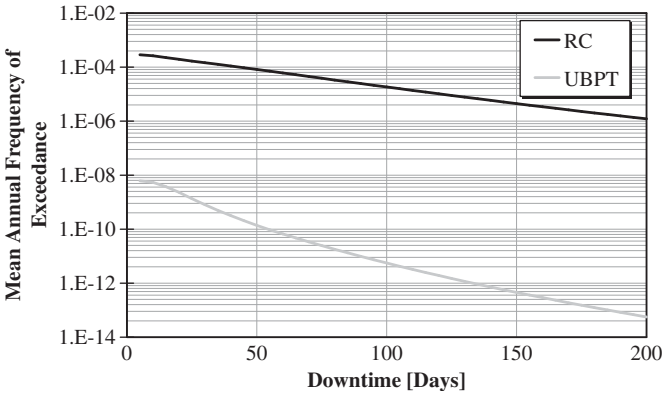

Figure 12. Hazard curves for downtime related to bridge demolition and replacement.

IDA results were slightly higher for the UBPT system. The UBPT system performed well, as the expected repair costs due to drift-related damage are similar to that of the RC system.

When comparing the downtime hazard curves for the two bridges, the mean annual frequency of exceedance of the UBPT system for a given value of downtime is significantly lower than that of the RC system. For example, for a downtime of 30 days, the RC system has a mean annual frequency of exceedance of approximately 1.5E-4, which corresponds to a probability of 0.75% in 50 years. In comparison, for a downtime of 30 days, the UBPT system has a mean annual frequency of exceedance of approximately 8.0E-10, which corresponds to a probability of only 0.000004% in 50 years. With increasing values of downtime, the difference between the two systems increases. The values for the UBPT system are so low that they can be considered to be essentially zero.

Considering the analysis results of the RC system alone allows for a benchmarking of a typical California overpass bridge designed according to current code. In terms of peak drifts at the 2% in 50 year intensity level, the RC bridge experiences a median value of roughly 2.6%, which corresponds to a ductility demand of less than 3. In terms of residual drifts at the same intensity level, the bridge sustains a median value of 0.6%. These values can be considered acceptable structural performance for a 2% in 50-year intensity level. A repair cost of $6800 for the RC bridge is expected with a probability of 2% in 50 years. The downtime expected with a probability of 2% in 50 years was less than 1 day. This code-conforming RC bridge therefore performs very well. For a bridge of great importance (for example along a major transportation artery), it may be desirable to have an expected downtime of essentially zero, which could be provided with UBPT columns.

The results from the comparative analysis provide an assessment of the performance of the UBPT system relative to the RC system. This quantitative performance assessment can be used to decide whether the use of the UBPT system is warranted for this bridge design. Based on these results, UBPT could be considered advantageous for this design in cases where the bridge is critical to the transportation network and a very low probability of experiencing downtime is desired.

CONCLUSIONS

RC highway bridges designed to current seismic design codes are expected to experience high inelastic deformation demands in their columns during large earthquakes, leading to the possibility of large residual displacements and therefore reduced post-earthquake functionality. A system for providing self-centering to the columns through the use of vertical, UBPT is proposed for use in highly seismic regions to improve post-earthquake functionality. Two benchmark highway bridge structures, using either conventional or self-centering systems, were modeled and evaluated quantitatively using a probabilistic, performance-based earthquake engineering (PBEE) assessment methodology.

DOI: 10.1002/eqe

From the structural analyses, the bridge with self-centering columns was found to perform well, sustaining similar peak drift demands as compared with the bridge with conventional columns, but with significantly reduced residual deformations. From the full PBEE analysis, the UBPT bridge was found to have similar expected repair costs to the RC bridge, due to the fact that the bridges had similar peak drift responses. The reduced residual displacements in the UBPT bridge were found to translate into significantly reduced expected downtime losses that would normally arise due to the required demolition and replacement of permanently deformed columns. The conventional RC bridge was found to perform well, and had a relatively low probability of exceeding a moderate amount of downtime. For example, for a downtime of 30 days, the mean annual frequency of exceedance for the RC bridge corresponded to a 0.7% probability in 50 years. The value for the UBPT bridge was essentially zero percent. The lower value of likely downtime for a UBPT system could be warranted for an important, highly traveled bridge.

The power of a PBEE assessment methodology is demonstrated in this study, in that a systematic and quantitative comparison is made between two competing structural systems that allows for more informed decision making, which incorporates a better understanding of post-earthquake functionality. Benefits of a new structural system (in this case the UBPT system) are also able to be demonstrated using the PBEE assessment methodology not only in terms of engineering response (i.e. reduced residual displacements), but also in terms of response that is easily understood by structure owners and to society in general (i.e. reduced structure downtime and therefore reduced disruption to the transportation network).

Certain challenges are present in the PBEE analysis of new types of structural systems such as the UBPT column system. For example, the lack of available data and subjectivity in damage states is a common obstacle that will be faced when developing fragility curves for the PEER PBEE framework when new systems or materials are considered. Additional studies should be performed to determine the extent of the sensitivity of the final results to assumptions that are made as well as to determine what areas may require future study. Future work should consider alternate bridge configurations (e.g. skew, differing column heights, multiple column bents, curved bridges) as well as improving modeling aspects such as incorporating soil–structure interaction and non-uniform support excitation.

NOTATION

The following symbols are used in this paper:

$v(DV)$	mean annual frequency of exceeding a certain DV
$G\langle DX\|DY\rangle$	the complementary CDF of DX conditioned on DY

ACKNOWLEDGEMENTS

This research was sponsored by the Earthquake Engineering Research Centers Program of the National Science Foundation through the Pacific Earthquake Engineering Research Center. The opinions expressed in this paper are those of the authors and not necessarily of the sponsor. Assistance with ground motion selection and Probabilistic Seismic Hazard Analysis from Dr Polsak Tothong is gratefully acknowledged.

REFERENCES

1. Kawashima K, MacRae G, Hoshikuma J, Nagaya K. Residual displacement response spectrum. *Journal of Structural Engineering* 1998; **124**(5):523–530.
2. Bazzurro P, Cornell C, Menun C, Motahari M. Guidelines for seismic assessment of damaged buildings. *Proceedings of the 13th World Conference on Earthquake Engineering*, Vancouver, Canada, 2004.
3. Luco N, Bazzurro P, Cornell C. Dynamic versus static computation of the residual capacity of a mainshock-damaged building to withstand an aftershock. *Proceedings of the 13th World Conference on Earthquake Engineering*, Vancouver, Canada, 2004.
4. Mackie K, Stojadinovic B. Residual displacements and post-earthquake capacity of highway bridges. *Proceedings of the 13th World Conference on Earthquake Engineering*, Vancouver, Canada, 2004.

DOI: 10.1002/eqe

5. Moehle J, Deierlein G. A framework methodology for performance-based earthquake engineering. *Proceedings of the 13th World Conference on Earthquake Engineering*, Vancouver, Canada, 2004.
6. Caltrans A. *Seismic Design Criteria V. 1.2*, California Department of Transportation, CA, U.S.A., 2001.
7. Ketchum M, Chang V, Shantz T. Influence of design ground motion level on highway bridge costs. *PEER Technical Report D601*, Pacific Earthquake Engineering Research Center, University of California, Berkeley, CA, 2004.
8. Sakai J, Mahin S. Hysteretic behavior and dynamic response of re-centering reinforced concrete columns. *Proceedings of the 6th Symposium on Seismic Design of Bridge Structures Based on the Ductility Design Method*, Tokyo, Japan, 2003.
9. Sakai J, Mahin S. Analytical investigations of new methods for reducing residual displacements of reinforced concrete bridge columns. *PEER Report 2004/02*, Pacific Earthquake Engineering Research Center, University of California, Berkeley, CA, 2004.
10. Sakai J, Jeong H, Mahin S. Earthquake simulator tests on the mitigation of residual displacements of reinforced concrete bridge columns. *Proceedings of the 21st U.S.–Japan Bridge Engineering Workshop*, Japan, 2005.
11. Abrahamson NA, Silva WJ. Empirical response spectral attenuation relations for shallow crustal earthquakes. *Seismological Research Letters* 1997; **68**(1):94–127.
12. Mackie K, Stojadinovic B. Seismic demands for performance-based design of bridges. *PEER Report 2003/16*, Pacific Earthquake Engineering Research Center, University of California, Berkeley, CA, 2003.
13. Scott M, Fenves G. Plastic hinge integration methods for force-based beam–column elements. *Journal of Structural Engineering* 2006; **132**(2):244–252.
14. Mander J, Priestley M, Park R. Seismic design of bridge piers. *Research Report 84-02*, University of Canterbury, Christchurch, New Zealand, 1983.
15. Scott B, Park R, Priestley M. Stress–strain behavior of concrete confined by overlapping hoops at low and high strain rates. *Journal of the American Concrete Institute* 1982; **79**(1):13–27.
16. Jeong HI, Mahin SA, Sakai J. Shaking table tests and numerical investigation of self-centering reinforced concrete bridge columns. *PEER Report 2008/06*, Pacific Earthquake Engineering Research Center, University of California, Berkeley, CA, 2008.
17. Hachem MM, Mahin SA, Moehle JP. Performance of circular reinforced concrete bridge columns under bidirectional earthquake loading. *PEER Report 2003/06*, Pacific Earthquake Engineering Research Center, University of California, Berkeley, CA, 2003.
18. Lee WK, Billington SL. Modeling residual displacements of concrete bridge columns under earthquake loads using fiber elements. *Journal of Bridge Engineering* 2010; **15**(3):240–249.
19. Taucer F, Spacone E, Filippou F. A fiber beam–column element for seismic response analysis of reinforced concrete structures. *UCB/EERC Technical Report 91/17*, Earthquake Engineering Research Center, University of California, Berkeley, 1991.
20. Lee WK, Billington SL. Simulation and performance-based earthquake engineering assessment of self-centering post-tensioned concrete bridge systems. *Blume Center Technical Report 159*, John A. Blume Earthquake Engineering Center, Stanford University, Stanford, CA, 2007.
21. Somerville P, Collins N. Ground motion time histories for the I880 Bridge–Oakland. *PEER Technical Report*, Pacific Earthquake Engineering Research Center, University of California, Berkeley, CA, 2002.
22. Vamvatsikos D, Cornell C. Incremental dynamic analysis. *Earthquake Engineering and Structural Dynamics* 2002; **31**(3):491–512.
23. Berry M, Eberhard M. Performance models for flexural damage in reinforced concrete columns, *PEER Report 2003/18*, Pacific Earthquake Engineering Research Center, University of California, Berkeley, CA, 2003.
24. Japan Road Association, *Specifications for Highway Bridges*. Japan Road Association: Japan, 2006.
25. Porter KA. An overview of PEER's performance-based earthquake engineering methodology. *Proceedings of the 9th Conference on Applications of Statistics and Probability in Civil Engineering*, San Francisco, CA, 2003.
26. Mackie K, Wong JM, Stojadinovic B. Method for post-earthquake highway bridge repair cost estimation. *Proceedings of the 5th National Seismic Conference on Bridges and Highways*, San Mateo, CA, 2006.
27. Caltrans. Construction Statistics Based on Bid Openings, California Department of Transportation, 2004. Available from: http://www.dot.ca.gov/hg/esc/estimates/Construction_Stats_2004.xls.
28. Caltrans. Bridge Design Aids—Section 11: Estimating, California Department of Transportation, 2005. Available from: http://www.dot.ca.gov/hq/esc/techpubs/manual/bridgemanuals/bridge-design-aids/bda/html.
29. FEMA. *HAZUS99 Service Release 2 Technical Manual*, Federal Emergency Management Agency, Washington, DC, U.S.A., 1999.

DOI: 10.1002/eqe